Title
Regulation of Developmental Angiogenesis by Collagen XVIII alpha 1

Author
Martinez, Julie

Publication Date
2023

Peer reviewed|Thesis/dissertation

UNIVERSITY OF CALIFORNIA

Los Angeles

Regulation of Developmental Angiogenesis by Collagen XVIII alpha 1

A thesis submitted in partial satisfaction

of the requirements for the degree Master of Science

in Physiological Science

by

Julie Martinez

2023

ABSTRACT OF THE THESIS

Regulation of Developmental Angiogenesis by Collagen XVIII alpha 1

by

Julie Martinez

Master of Science in Physiological Science

University of California, Los Angeles, 2023

Professor Pearl Jennine Quijada, Chair

Background:

Myocardial infarctions (MI) are a leading cause of death worldwide. Unfortunately, the adult heart cannot generate new vessels after MI leading to impaired myocardial perfusion and function. This study aims to identify reprogramming factors during embryonic angiogenesis, which may enhance neovascularization in the adult heart after MI. Our lab discovered 56 novel secreted ligand genes expressed by epicardial cells during development. One factor, collagen, type XVIII, alpha 1 (*Col18a1*), an angiogenesis inhibitor, has not been thoroughly investigated in the heart.

Methods:

Wilm's tumor gene 1 (Wt1) transgenic and C57BL/6 mouse strains were used to investigate *Col18a1* expression at embryonic (E) and early post-natal (P) time points. Overexpression of COL18A1 in the epicardium was performed at E12.5 to investigate alterations in coronary angiogenesis using gene expression and immunohistochemical analyses.

Results:

Col18a1 increased in Wt1+ epicardial cells during coronary vasculature formation, peaking at E16.5, and stabilized during the early postnatal periods determined by fluorescence *in situ* hybridization assays. Gene expression data was corroborated following immunohistochemical analysis of endostatin, a proteolytically produced C-terminal fragment of COL18A1 and potent antiangiogenic protein. COL18A1 overexpression in the developing epicardium caused a dysregulation of endothelial cell (EC) positioning within the epicardium, observed after immunolabeling for ERG+ cells. Gene expression data confirmed dysregulation of EC differentiation with a downregulation in arterial *Nrp1* and upregulation of venous *Nr2f2*.

Conclusions:

Our data suggest that mRNA and protein levels of *Col18a1* and endostatin increased during embryogenesis to limit coronary angiogenesis. Overexpression of COL18A1 inhibited migration and preserved a venous and coronary plexus phenotype in ECs. Furthermore, overexpression of COL18A1 produced immature and proliferative epicardial cells, confirmed by an upregulation in epithelial-to-mesenchymal genes. We theorize that inhibition of epicardial cell differentiation by COL18A1 overexpression drives the dysregulation in EC placement and coronary development.

The thesis of Julie Martinez is approved:

Amy Catherine Rowat

Patricia Emory Phelps

Pearl Jennine Quijada, Committee Chair

University of California, Los Angeles

2023

DEDICATION

This thesis would not be complete without the help from my loved ones. Dad, you have been the constant support I needed to keep going in times of adversity. Mom, if it weren't for your uplifting words of encouragement since the very beginning, I am not sure if I would have walked through the front door of my first class. Lezlie, thank you for constantly being there to remind me the world is not ending, and reminding me that I will be, where I need to be. Lastly, Cole, words cannot describe the gratitude I have for having your support throughout my entire academic journey, you have been there to celebrate all my highs and lows and I wouldn't want it any other way.

TABLE OF CONTENTS

LIST OF FIGURES

ABBREVIATIONS

ARC	Animal Research Committee
BGal	β-Galactosidase
CD31	Cluster of Differentiation 31
Col18a1	Collagen, type XVIII, alpha one
DLAM	Division of Laboratory Animal Medicine
DepC	Diethyl Pyrocarbonate
EMT	Epithelial to Mesenchymal Transition
EPDCs	Epicardium-Derived Progenitor Cells
FACS	Fluorescence-Activated Cell Sorting
FBS	Fetal Bovine Serum
FFPE	Formalin-Fixed, Paraffin-Embedded
FGF-2	Fibroblast Growth Factor 2
FISH	Fluorescence *in situ* Hybridization
FN	Fibronectin
HRP	Horseradish Peroxidase
IHC	Immunohistochemistry
LV	Left Ventricle
MI	Myocardial Infarction
MMP-2	Matrix Metalloproteinase
NBF	Neutral Buffered Formalin
PDGF	Platelet-Derived Growth Factor
RT	Room Temperature
SSC	Saline Sodium Citrate
TCF21	Transcription Factor 21
TGF-β	Transforming Growth Factor β
TPCL	Translational Pathology Core Laboratory
TSA	Tyramide-Signal Amplification
VEGF	Vascular Endothelial Growth Factor
WT1	Wilm's Tumor 1
1x TN	150 mM NaCl/100 mM Tris pH7.5

ACKNOWLEDGMENTS

I would like to thank my mentor, Dr. Pearl Quijada, for providing immense guidance throughout this insane journey. You have taught me how to become a scientist and to never give up on myself. You have inspired me to keep chasing my career aspirations, unconditional of how insane they may feel. Thank for teaching me how to be a role model to others. Lastly, I credit you for keeping my curiosity candle bright and lit.

I would also like to thank Maya Cielo Cornejo and Matthew Tran who were always there for me day in and day out. Maya, thank you for sitting through hours of experiments just so I would have someone to talk my ideas through. Thank you for being there for me when I faced weeks of failed experiments and reminding me that science requires a bit of failing to succeed. Matthew, thank you for your unwavering kindness and joy; even on our toughest of days you always knew how to make us all laugh. I also want to thank you for proofreading every document I submitted during my master's degree. I consider myself lucky to have been surrounded by Maya and Matthew.

Thank you to all the members of the Quijada Lab. It was through your constant support and kindness that I was able to survive the difficulties in my project. I am honored to have spent these past two years surrounded by such inquisitive and intellectual minds.

This study was made possible by the following grants: UCLA Start-Up Fund, BSCRC Innovation Award, and the AHA Career Development Award.

BACKGROUND

Heart disease is currently the leading cause of death [3] in the United States, with myocardial infarctions (MI) being one of the most common subtypes, with annual incidence rate of 805,000 in the United States [24]. MI is caused by the blockage of blood flow to the heart, typically caused by a buildup of atherosclerotic plaques resulting in the loss of functional vasculature and myocardium and progression to severe chronic ventricular failure and dysfunction [6]. Though there remains an overall loss of function vasculature, studies have shown that the heart has an endogenous tissue repair mechanism following MI, including acute angiogenesis in the infarct region stimulated by increases in vascular endothelial growth factor (VEGF) and hypoxia [27]. While current treatments address the immediate blockage of the vasculature around the heart [6], they do not consider long-term treatment options. One alternative approach to vascular repair considers the induction of angiogenesis or the formation of new blood vessels from preexisting vessels. Clinical trials have considered VEGF as a candidate factor for protein therapy to induce angiogenesis following MI, but patients only experienced modest perfusion [20]. Studies like those discussed above show that stimulatory growth factors, such as VEGF, alone are insufficient to serve as a treatment for MI. Cardiac vessels are primarily formed during embryonic development, and adult hearts cannot remodel existing vasculature or generate new vessels following any injury, including MI. By studying the factors that regulate and influence coronary angiogenesis during stages of development, we may obtain better insight into novel therapeutics following MI.

Heart Development-

The heart is the first organ to fully develop in an embryo [5]. In mice, heart development begins at embryonic (E) day 7.5 with the cardiac crescent formation. At E9.5, proepicardium-derived cells will start to take part in a migratory event and attach to the atrioventricular canal of the nascent heart, thus forming a single layer of mesothelium-derived cell layer known as the epicardium [15]. The epicardium is considered developed by E12.5, but the heart requires extended time to fully mature at E16.5 [15].

This single layer of the epicardium is critical in the development of the heart. It is a rich source of various cell types, such as cardiac fibroblasts, mural cells, and paracrine signals [9, 15]. The epicardium can influence and enable embryonic cardiomyocyte maturation and coronary vasculature formation through its involvement in a cellular process called epithelial-to-mesenchymal transition (EMT). Indeed, genetic ablation experiments of the epicardium have led to catastrophic defects in coronary vasculature formation, indicating that the epicardium instructs important morphogenetic events.

EMT is a cellular process in which epithelial cells lose their apical-basal polarity and cell-cell adhesion properties and acquire migratory and invasive characteristics commonly observed in mesenchymal stem cells [7-8]. EMT is most active at E14.5 and will result in cells moving toward the subepicardial mesenchyme of the myocardium as they differentiate into various subtypes of cells. The cells that arise from this process are known as epicardium-derived progenitor cells (EPDCs). EPDCs contribute to the formation of coronary vasculature in the heart, a process known as coronary angiogenesis. Secreted ligands influence the formation of

new blood vessels by the epicardium, the composition of the extracellular matrix, and growth factors bound to the extracellular matrix.

Analyzing previous single-cell RNA sequencing of the developing epicardium, my lab discovered 56 novel secreted ligand genes expressed by epicardial cells during embryonic angiogenesis [16]. One of the genes identified in this study, *Col18a1* [16], has been previously shown to inhibit angiogenesis [11-13] through the cleavage of the C-terminal domain of *Col18a1.* Cleavage results in a product called endostatin, which has numerous molecular mechanisms contributing to its anti-angiogenic effect. Endostatin can block the activation and catalytic activity of matrix metalloproteinase 2 (MMP-2) [17], a key enzyme for biological processes such as angiogenesis [25]. It may also interfere with vascular growth signals initiated by pro-angiogenic signaling pathways such as Vascular endothelial growth factor (VEGF) and Fibroblast Growth Factor 2 (FGF-2). Although several lines of evidence support *Col18a1* as an angiogenesis inhibitor, its role in the epicardium and coronary vasculature formation has not been previously defined.

This project aims to characterize further *Col18a1*'s role in the developing heart, a period in which coronary angiogenesis is predominant. I hypothesize that Col18a1 regulates embryonic angiogenesis, and the artificial overexpression of COL18A1 in the embryonic heart will alter EMT and, therefore, EC placement and differentiation. To further characterize *Col18a1*, I will evaluate the expression in epicardial cells during embryonic development (embryonic day 12.5 to 16.5) and the postnatal period (postnatal days 1 to 10). In addition, I will identify the role of COL18A1 in the epicardium and its influence on coronary vasculature formation.

CHAPTER 1: DEFINING THE EXPRESSION PATTERNING OF COLLAGEN VXIII ALPHA ONE DURING EMBRYONIC AND EARLY POSTNATAL DEVELOPMENT

Introduction

The circulatory system consists of two main components: the heart and a network of vessels, which together, deliver oxygen and other nutrients to various body parts making this system critical to the survival an organism. The myocardium and epicardium must be developed during the first stages of embryonic development. The proepicardium is a transient extracardiac embryonic tissue rich in progenitor cells [15]. The proepicardium will give rise to the epicardium with the maturation of the epicardium at E12.5. With mature epicardium formed, coronary vasculature development can begin with the recruitment of immature endothelial cells followed by endothelial cell differentiation towards artery or venous cells fates [18]. Endothelial cells localized in the sub-epicardium express venous cell fates, whereas endothelial cells in the compact myocardium will become arteries [18].

Epithelial-to-mesenchymal transition (EMT) is a critical process for coronary vasculature development and must be highly regulated for proper cardiac development. EMT allows cellular migration and differentiation to occur and can be regulated by the expression of transcription and growth factors [8]. Transcription factors are proteins that aid RNA transcription from template DNA by regulating gene expression. To induce EMT, transcription factors such as SNAIL, SLUG, ZEB1, and TWIST1, repress epithelial adhesion genes and activate mesenchymal genes [2, 8], and then promote the migration and the production of the extracellular matrix. Growth factors supplement EMT-inducing transcription factors. They are signaling proteins that stimulate cell differentiation, cellular proliferation, tissue repair, and inflammation. The two

most common growth factors shown to regulate EMT are transforming growth factor β (TGF-β) [28] and platelet-derived growth factor (PDGF) [1].

Work conducted by Compton et al. showed that epicardial explants stimulated with TGF-β lose their epithelial markers and upregulate mesenchymal markers, specifically in smooth muscle cells [4]. Like TGF-β, PDGF is a molecule that binds to the receptor tyrosine kinase that regulates EMT and epicardial-derived cell (EPDC) specification. Studies by Smith reported that epicardial cells null for PDGF receptors were unresponsive to pro-EMT stimulation and expressed low levels of EMT-inducing transcription factors and mesenchymal genes [21]. Both studies show that without these growth factors, the cells will not go through EMT, and hearts lack functional coronary vasculature.

With the completion of EMT at E 16.5, the mural heart is now considered mature and morphologically complete. However, even after birth, the heart displays an ability to regenerate. As demonstrated through work conducted by Porrello et al [14]. Before their work, it was thought that the heart did not regenerate after birth in mammals but was evolutionarily conserved in amphibians. To test the heart's capacity to regenerate after birth, researchers surgically resectioned the apex of the mural neonatal heart at postnatal (P) day 1. They evaluated the heart with serial histological analysis. They noted that at P21, the location of the apex resection appeared to be replaced with normal myocardial tissue demonstrating regeneration. The authors were then interested to see if the regenerative property was still seen after the cardiomyocytes withdrew from the cell cycle at P7. After repeating this study, the authors concluded that the mice failed to regenerate the apex of the heart and developed significant fibrosis, thus identifying a period of regeneration after birth as P1 – P7.

Given the various regulatory factors involved in coronary vasculature development, I want to investigate an underappreciated secreted ligand factor, COL18A1. As an anti-angiogenic factor, the role *Col18a1* plays in vasculature growth requires further investigation. Doing so may provide further insight into the mechanisms vital to vasculature development and regeneration.

Materials and Methods

Animals

Mice were housed in the University of California – Los Angeles Terasaki Life Sciences Building and were housed in accordance with Animal Research Committee (ARC) and Division of Laboratory Animal Medicine (DLAM) standards. All animal experiments were approved by the University of California – Los Angeles and held to ethical regulations for research and testing.

This study used mice purchased from The Jackson Laboratory. These mice were maintained with a C57BL/6J background (stock # 664). Rosa26R$^{mTmG/mTmG}$ mice were purchased from The Jackson Laboratory (stock # 7676). Rosa26^{tdTomato} mice were purchased from The Jackson Laboratory (stock # 7909). Wt1$^{CreERT2/+}$ mice were purchased from The Jackson Laboratory (stock # 10912).

These mice were bred to carry a fluorescent reporter through the tamoxifen-inducible Cre Lox crossed with Rosa26R$^{mTmG/mTmG}$ or Rosa26^{tdTomato}. This Cre-based system allows for labeling epicardial cells positive with Wilm's Tumor Gene and epicardial-derived cells. To time pregnancies, breeding was set up with one male with one or two females in a single cage. The

following morning, females were checked for copulatory plugs and separated, with any confirmed plugs being E 0.5.

Tamoxifen induction was administered according to individual experiments along with embryonic isolation. The breeding strategy for embryos planned for quantitative PCR, immunostaining, and in situ hybridization goes as follows. Rosa26R$^{mTmG/mTmG}$ females were crossed with Wt1$^{CreERT2/+}$ males. 4-Hydroxytamoxifen (4-OHT) (Sigma-Aldrich, Catalog No. H6278-50MG) was dissolved in sunflower seed oil from *Helianthus annuus* (Sigma-Aldrich, Catalog No. S5007-250ML) with 200 Proof ethanol to a final concentration of 10 mg/mL. 4-OHT was administered to pregnant dams at E 9.5 and E 10.5 via oral gavage at 75 mg/kg. Embryos were isolated at E12.5, E14.5, and E16.5. The breeding strategy for neonates planned to be used for quantitative PCR, immunostaining, and in situ hybridization goes as such. Rosa26^{tdTomato} females were crossed with Wt1$^{CreERT2/+}$ males. 4-Hydroxytamoxifen (4-OHT) was dissolved in sunflower seed oil from *Helianthus annuus* with 200 Proof ethanol to a final 25 mg/mL concentration. 4-OHT was administered at P1 to neonates via subcutaneous injections at 12.5 mg/kg. Neonatal hearts were isolated at P2, P4, P7, and P10.

Heart Isolation

Heart isolations were conducted according to individual experiments and their corresponding time courses. Following isolation, hearts were processed by the Translational Pathology Core Laboratory (TPCL) at UCLA or digested with intention of isolating RNA for quantitative PCR analysis.

Embryonic Isolations

Pregnant dames were anesthetized with 0.5 mL of ketamine-xylazine cocktail (13 mg/mL ketamine and 0.88 mg/mL xylazine in DPBS) via intraperitoneal injection. Upon anesthetization, the pregnant dams were sacrificed using cervical dislocation. The abdominal area was sterilized with 70% ethanol. Following, a lateral incision was made with straight surgical scissors to expose the abdominal cavity. Decidua was then removed from the mesometrium and placed in pre-warmed HBSS (ThermoFisher Scientific, Catalog No. MT21021CM). Extra embryonic tissues and the yolk sacks were removed from the embryos. Embryos were then decapitated, and hearts were removed. Hearts being sent off to TPCL were fixed in 10% Neutral Buffered Formalin (NBF) (ThermoFisher Scientific, Catalog No. 22-110-869) for four hours and then in 70% histology-grade ethanol (ThermoFisher Scientific, Catalog No. 22-050-106). Hearts being used with the intention of RNA isolation were minced with dissection scissors and placed in 800µL of TRIzol.

Neonatal Isolations

Neonatal pups were anesthetized via hypothermia and were sacrificed using decapitation. Following, an incision was made along the sternum with straight surgical scissors to expose the chest cavity and heart. The heart was extracted with curved forceps. Hearts being sent off to Translational Pathology Core Laboratory (TPCL) were then placed in 10% NBF (ThermoFisher Scientific, Catalog No. 22-110-869) for four hours and then placed in 70% histology grade ethanol (ThermoFisher Scientific, Catalog

No. 22-050-106). Hearts being used with intention of RNA isolation were minced with dissection scissors and placed in 800µL of TRIzol.

RNA Isolation, cDNA biosynthesis, and quantitative PCR

RNA was isolated from minced hearts with TRIzol. Chloroform was added to each sample and shaken vigorously to distribute the chloroform with the sample evenly. Each sample was centrifuged at 13 000 rpm for 15 minutes at 4ºC. The aqueous layer was then removed and put into a separate Eppendorf tube, as this is the layer with the RNA of interest. An equal volume isopropanol and 10 µg of glycogen (ThermoFisher Scientific, Catalog No. 10814010) were added to the Eppendorf tubes, inverted 6-8 times, then incubated for 10 minutes on ice. Samples were then centrifuged at 13 000 rpm for 10 minutes at 4ºC. Isopropanol was removed without disturbing the RNA pellet. 1 mL of 75% ethanol in DepC-treated H_2O was added to begin the rinsing process. Each sample was centrifuged at 13 000 rpm for 5 minutes at 4ºC. Any remaining ethanol was then removed and air dried for 20 minutes. Diethyl pyrocarbonate (DepC) H_2O (12 µL for embryonic hearts and 20 µL for neonatal hearts) was then added to resuspend the pellet before measuring RNA quantity with the NanoDrop200.

Purified RNA was made into cDNA using the Thermo Scientific™ Verso cDNA Synthesis Kit. To run a gene expression analysis, qRT-PCR was conducted with cDNA using the primers stated (Table 3) and the SSO Advanced Universal SYBR Green. Data were analyzed using the $\Delta\Delta C(t)$ method but samples with abnormal melt curves were not used for analysis.

Immunohistochemistry

Hearts from $Wt1^{CreERT2/+}$; $Rosa26R^{mTmG/mTmG}$ (E12.5, E14.5, and E16.5), and $Wt1^{CreERT2/+}$; $Rosa26^{tdomato}$ (P2, P4, P7, and P10) were harvested and sent to TPCL for paraffin embedding and sectioning (5 μm thick). Slides were baked in the hybridization oven for one hour at 60ºC. Slides were then deparaffinized by submerging in a series of xylenes and alcohols (xylene solution for five minutes three times, absolute alcohol for three minutes three times, 95% alcohol for 3 minutes two times, 70% alcohol for three minutes once). Samples were rehydrated with distilled water for five minutes. Antigen retrieval was performed with 1X antigen retrieval buffer diluted (Akoya Biosciences, Catalog No. AR600250ML) from a 10X stock solution with distilled water. Samples then had their endogenous tissue quenched for HRP conjugated secondaries with 3% H_2O_2 diluted in 150mM NaCl/100mM Tris pH7.5 (1X TN) for 20 minutes. Opal antibody diluent block (Akoya Biosciences, Catalog No. ARD1001EA) was used to block the non-specific binding of antibodies with an incubation period of 30 minutes. Primary antibodies were diluted in opal antibody diluent, as stated in Table 1 and incubated overnight at 4ºC. Primary antibodies were washed with 1X TN for five minutes three times. Secondary antibodies were diluted in Opal antibody diluent, as stated in Table 1 and incubated at room temperature for 2 hours. For samples that required amplification, a tertiary opal antibody was added according to the dilution rate stated in Table 1 and incubated for 10 minutes. All opal amplifications were diluted in amplification dilution buffer (Akoya Biosciences, Catalog No. FP1498). Following incubation, slides were washed in 1X TN for five minutes three times. On the final wash, DAPI (BD Biosciences, Catalog No. 564907) (1mg/mL) was diluted in 1X TN at a dilution of 1: 10 000. Slides were mounted with Prolong Gold anti-fade mounting media

(Fisher Scientific, Catalog No. P36930) prior to being coverslipped (Genesee Scientific, Catalog No. 29-118). Imaging of slides was conducted on the Zeiss LSM 700 Confocal and Zeiss LSM 880 Confocal with Airyscan.

Fluorescent In Situ Hybridization

Hearts from $Wt1^{CreERT2/+}$; $Rosa26R^{mTmG/mTmG}$ (E12.5, E14.5, and E16.5), and $Wt1^{CreERT2/+}$; $Rosa26^{Tomato}$ (P2, P4, P7, and P10) were harvested and sent to TPCL for sectioning (5 μm thick) and paraffin embedding. mRNA labeling was conducted using of RNAscope Protease Multiplex Fluorescent Reagent Kit v2 Assay and following the user's manual for formalin-fixed, paraffin-embedded (FFPE) tissue with minor modifications. A manual antigen retrieval was performed for ten minutes, and RNAscope Protease Plus was incubated on the slides for thirty minutes. All pretreatment protocols were followed prior to a combination of 2-3 mRNA probes (Table 2) and were hybridized for two hours at 40ºC. Samples were stored at room temperature in 5X Saline Sodium Citrate (SSC) overnight. The following day, all probes were amplified and developed with horseradish peroxidase (HRP) for C1, C2, or C3 conjugated probes. Following HRP development, opals diluted in Tyramide-Signal Amplification (TSA) (ACD Bio, Catalog No. 323270) were added to fluorescently label each corresponding probe. DAPI (ACD Bio, Catalog No. 323270) was added to each section before mounting slides with prolonged gold and cover slipping. Slides were imaged on the Zeiss LSM 700 Confocal and Zeiss LSM 880 Confocal with Airyscan.

Statistical Analysis

Bar graph data was presented and analyzed using a mean ± SEM. An unpaired two-tailed student t-test and one-way ANOVA was used for data analysis. Bar graph analysis was performed on Graph Pad Prism. A p-value of <0.05 was considered significant.

Results

Prior work has elucidated the role of secreted ligands in coronary angiogenesis and EMT, which temporally overlap between the days of E12.5 and E16.5. As previously stated, little information is known about the role of *Col18a1* and its endogenous temporal-spatial localization within the developing heart. To further characterize the role of *Col18a1*, transgenic mouse models were generated to label Wilm's Tumor 1-positive cells with the fluorescent marker, GFP, following tamoxifen induction (Fig 1.1 A - C). Wilm's Tumor 1 is highly expressed in the epicardium during heart development and downregulated during epicardial EMT. If a cell is WT1+ at the time of tamoxifen induction, the cell will express GFP and will continue to express GFP if differentiation is to occur, allowing for fate mapping. Pregnant dams were administered 4-OHT (a tamoxifen analog) at E9.5 and E10.5, allowing for epicardial cells to express GFP at E12.5. As these epicardial cells went through EMT, they continued to express GFP even if they no longer were WT1+ (Fig 1D). Conversely, neonates were given 4-OHT at P1. As EMT has already occurred by this time, WT1+ cells are only seen on the epicardium in postnatal hearts (Fig. 1 H-K). *Col18a1* levels were visualized with FISH. At earlier time points, *Col18a1* originating from the epicardium is seen in low abundance but increases in fluorescence as the heart develops, with a peak in expression at E16.5 (Fig. 1.2 A-C). In the postnatal period,

Col18a1 is seen to stabilize expression throughout the myocardium (Fig 1.2 D-G). *Tcf21,* a marker for epicardial cells and epicardial-derived fibroblasts, is seen in low abundance at the epicardium at E12.5 and increases in fluorescence as the heart matures (Fig. 1.2 A-G). In addition, *Tcf21* and *Col18a1* migrates toward the endocardium starting at E14.5 (Fig. 1.2 A-G). *Col18a1*+ cell migration analysis of FISH images demonstrates a statistical significance in *Col18a1*+ cell placement between 0-10µm to 10-20µm, and 20-30µm distances from the epicardium at E12.5 (Fig. 1.2 H). We conducted a whole heart qPCR gene analysis of *Fibronectin* (Fn) and *Col18a1* to validate FISH mRNA findings. *Fn* was used as a positive control for our samples as it is known to be an ECM molecule that is highly abundant during development but declines in the postnatal heart (Fig 1.3 B). *Col18a1* is upregulated during embryonic development but downregulated during regeneration period (Fig 1.3A), further validating FISH expression analysis at the whole heart level. Though the characterization of *Col18a1* is insightful, knowing the localization of its active form, endostatin, may provide further insights into its role in heart development. As previously mentioned, endostatin is a C-terminal monomeric fragment of *Col18a1* and is characterized as anti-angiogenic. Like expression patterns seen with *Col18a1*, endostatin begins in low abundance at E12.5 but increases over time (Fig 1.4A). In contrast to *Col18a1* mRNA data, endostatin remains at the epicardium and colocalizes with WT1+ cells (Fig 1.4A).

Discussion

Before this study, the role of *Col18a1* in the developing heart remained unknown. Here we show that *Col18a1* originates from both the epicardium and endocardium layers of the heart. Although there is a presence of *Col18a1* in the endocardium, this study primarily focused on its role in the epicardium as it is a source of various cell types and paracrine signals critical for development. We hypothesize that *Col18a1* may guide coronary vasculature development as its abundance increases during periods of vascular growth but stabilizes once vasculature growth has been completed. Though it is understood that there is a period of regeneration during P1 to P10, we conclude that without injury, there is no need to maintain high levels of *Col18a1*. In addition, the same factors that allow for vasculature development may not remain active during the postnatal period without injury and, thus, do not need the regulation that *Col18a1* and endostatin may provide. To characterize the role of endostatin on coronary vasculature development, we will evaluate coronary angiogenesis using an *ex vivo* model of artificial overexpression of endostatin.

CHAPTER 2: DETERMINE THE EFFECTS OF ARTIFICIAL OVEREXPRESSION OF COL18A1 ON CARDIAC ANGIOGENESIS

Introduction

As previously discussed, developing coronary vasculature requires a large input from the epicardium. The epicardium provides secreted ligands that guide coronary vessel development and is the source of numerous cell types following EMT. It is important to note that EPDCs contribute to cell lineages such as cardiac fibroblasts, smooth muscle cells, and pericytes, all of critical to coronary vasculature maturation [15]. The endothelial cells that become veins and arteries originate from the sinus venous and endocardium [22, 26]. The formation of coronary arteries was first shown to arise from angiogenic sprouts from the sinus venosus, suggesting veins are progenitors of arteries [18]. This transition from immature venous cells to mature arterial cell fate is influenced by the genetic and mechanical states of the epicardium as paracrine signaling contributes to their formation [9, 19]. Work conducted by Trembley et. al. demonstrated a vital link between the epicardium and the health of coronary microvascular maturation [23]. Conditional deletion of *Mrtfa* and *Mrtfb* in epicardium disrupted cell migration, resulting in hemorrhages in the sub-epicardium due to the depletion of epicardial-derived mural cells. Through their study, Trembley et. al. demonstrated that EMT is required for proper coronary vasculature development. A previous study in our lab further supports the role of EMT in EC localization and cell fate specification. Our study identified the role of Slit2+ EPDCs as vascular guidepost cells, and conditional silencing of Slit2+ EPDCs led to a continued expression of immature EC phenotypes and hindered cell migration toward the sup-epicardium and myocardium [16].

Through studies like those discussed above, we hypothesize that COL18A1 in the epicardium is essential for EMT and coronary angiogenesis. We also hypothesize that artificial overexpression of COL18A1 will limit the migration of EPDCs and the differentiation of veins to arteries, which may result in a dysfunctional cardiac phenotype.

Materials and Methods

Animals

Mice were housed in the University of California – Los Angeles Terasaki Life Sciences Building and were housed in accordance with ARC and DLAM standards. All animal experiments were approved by the University of California – Los Angeles and held to ethical regulations for research and testing.

This study used mice purchased from The Jackson Laboratory. C57BL/6J mice were purchased from The Jackson Laboratory (stock # 664). To time pregnancies, breeding was set up with one male with one or two females in a single cage. The following morning, females were checked for copulatory plugs and separated, with any confirmed plugs being E 0.5. The breeding strategy for embryos planned to be used for quantitative PCR and immunostaining goes as such. C57BL/6J females were crossed with C57BL/6J males. Embryos were isolated at E 12.5.

Adenoviruses

Pregnant dams were sacrificed, and embryos were isolated, as previously described in Chapter 1. Embryos were sacrificed using decapitation and had their lower torso removed, starting at the liver. The remaining chest cavity was placed into a six-well dish containing low-melting agarose (Thermo Scientific, Catalog No. FERR0801). Upon placement, the left ribcage

was removed to expose the heart. Cell culture media (DMEM: M199 (Fisher Scientific, Catalog No. MT10017CV; Fisher Scientific, Catalog No. 11-150-059), 10% Fetal Bovine Serum (Fisher Scientific, Catalog No. SH3091003HI), and 1% Penicillin/Streptomycin (Fisher Scientific, Catalog No. SV30010)) containing adenoviruses to cause artificial overexpression of GFP (Vector Biolabs, Catalog No. 1060) and β-Galactosidase (BGal) (Vector Biolabs, Catalog No. 1080) or COL18A1 (Vector Biolabs, Catalog No.165590540200) were added to the exposed hearts to express their corresponding proteins on the epicardial surface. Hearts were incubated with infection for 24 hrs at 37ºC and 5% CO_2. Infection media was removed, and cell culture media (DMEM: M199, 10% FBS, and 1% P/S) containing TGF-β1 [10ng/mL] and PDGF-BB [20ng/mL] were added to induce EMT and were incubated for an additional 24 hours.

Heart Digestion and Endothelial Cell Isolation

Heart digestion began with removing the cell culture media off the hearts and adding media containing 0.08% Collagenase IV (Worthington Biochemical, Catalog No. LS004188), 0.05% Trypsin (Fisher Scientific, Catalog No. SH3004201), and 1% Fetal Bovine Serum (FBS) diluted in HBSS. Hearts were then placed into the hybridization oven at 37 °C for intervals of five minutes with gentle shaking. After each 5 minute interval, hearts were broken down by gently pipetting the tissue up and down. Intact tissue was left to settle, and media containing cells was then collected in a separate tube with FBS to neutralize the digestion media. Cells were filtered through a 40 μm filter for collection. These intervals were repeated four times to completely digest the hearts. The collected media was centrifuged at 4°C for 10 minutes at 1200 rounds per minute. The supernatant was aspirated, and the pellet was resuspended in 0.5% bovine serum albumin (Sigma-Aldrich, Catalog No. A9647-100G) in DPBS. CD31-APC (BD Biosciences; Catalog No. 551262) was added to resuspended cells at a concentration of 1:100 to

label endothelial cells, incubated for 30 minutes, and washed with 0.5% BSA. Resuspended cells were kept on ice until fluorescence-activated cell sorting (FACS) using the BD FACS ARIA II. Cells were sorted using the 100 μm nozzle. DRAQ5 was added to resuspended cells before sorting for the labeling of live cells. Cells were sorted into 1.5 mL Eppendorf tubes containing 0.5% BSA diluted in DPBS. Following collection, TRIzol was added into each Eppendorf tube to begin lysing the cells for RNA isolation.

RNA Isolation, cDNA Biosynthesis, and Quantitative PCR

RNA isolation, cDNA biosynthesis, and quantitative PCR were performed as previously discussed in Chapter 1. Primers from Table 3 were used to analyze gene expression, and the ΔΔC(t) method was used to identify fold changes between groups. Abnormal melt curves were not used for analysis.

Immunohistochemistry

Hearts from C57BL/6J embryos were harvested, exposed to adenoviruses as previously described, put through a sucrose gradient with a final concentration of 30% sucrose, frozen in OCT (Fisher Scientific, Catalog No. 23-730-571) according to experimental groups, and cryosectioned (10μm thick). Slides were thawed at RT for 10 minutes and hydrated in PBS for five minutes. To allow for the antibodies to attach to the samples, slides were permeabilized with 0.2% Triton X-100 in PBS for 10 minutes. After washing with PBS, samples were incubated with 10% donkey serum in PBS for 30 minutes to block the non-specific binding of antibodies. Primary antibodies were diluted in 10% donkey serum in PBS, as stated in Table 4, and incubated overnight at 4ºC. Primary antibodies were washed off with PBS for five minutes three

times. Secondary antibodies were diluted in 10% donkey serum in PBS, as stated in Table 4, and incubated at room temperature for 1.5 hours. Following incubation, slides were washed in PBS for five minutes three times. DAPI (1mg/mL) was diluted in PBS at a dilution of 1: 2,000 and added directly onto the slides for five minutes. Slides were mounted with Prolong Gold anti-fade mounting media prior to being coverslipped. Imaging of slides was conducted on the Zeiss LSM 700 Confocal and Zeiss LSM 880 Confocal with Airyscan.

Statistical analysis

Bar graph data was presented and analyzed using a mean ± SEM. An unpaired two-tailed student t-test and one-way ANOVA were used for data analysis. Bar graph analysis was performed on Graph Pad Prism. A p-value of <0.05 was considered significant.

Results

As previously discussed, the role of COL18A1 in the developing heart has yet to be identified. In the previous chapter, we focused on understanding the endogenous levels and localization of *Col18a1* and its protein endostatin. Here, we focus on identifying the role of COL18A1 on coronary vessel maturation through artificial overexpression with adenovirus in E12.5 hearts cultured *ex vivo* (Fig 2.1 A). Coronary vasculature development requires immature venous ECs to migrate toward the sub-epicardium, which later differentiate into arterial fate as they infiltrate the myocardium. Treatment of *ex vivo* hearts with adenoviruses infects the first cell layer of the heart, specifically the epicardium with GFP and COL18A1-HA or GFP and BGal, which was used as a control adenovirus (Fig 2.1B). The adenovirus infection was

maintained for 24 hours and was followed by 24-hour incubation with EMT-inducing media (TGFβ1 and PDGF-BB). Hearts were then sectioned or digested to isolate CD31+ and CD31-, endothelial and non-endothelial cell sorting, respectively via FACS, followed by gene expression assays evaluated by qPCR (Fig 2.1 A). Col18A1-HA overexpression was validated by labeling hearts with an anti-HA antibody using IHC (Fig 2.1 B). E-26 transformation-specific related gene (ERG) is a transcription factor commonly found in endothelial cells. Immunolabeling for ERG+ cells shows that ECs are primarily found in the myocardium, which is expected at this developmental age (Fig 2.2). However, EC migration appears inhibited following AD-COL18A1- HA exposure as visualized by ERG+ cells in the subepicardial space (Fig 2.2 B). These results lead us to further investigate the EC dysregulation by studying gene expression changes. Col18A1-HA overexpression was validated by qPCR following CD31- and CD31+ cell sorting (Fig 2.3 A). Dysregulation of EC differentiation was confirmed in AD-COL18A1-HA exposed CD31+ cells with a down-regulation in *Nrp1*, an arterial marker, and upregulation in *Nr2f2*, a venous marker compared to BGal treated ECs (Fig 2.3 C-D). In addition, following AD-COL18A1 HA exposure, CD31+ cells showed an increase in *Cdk1*, a marker of cell proliferation and venous cell identity. In CD31- cells which include EPDCs among other cell types like cardiomyocytes, we found increases in EMT genes *Zeb2* compared to control cells. Finally, CD31+ and CD31- cells showed increased expression of *Apln* following *COL18A1* overexpression, which may be indicative of increased cellular immaturity as compared to control cells (Fig 2.3 B-F). These data suggest that COL18A1 is critical in coronary vasculature development, specifically cell specification and cell placement during coronary angiogenesis in the embryo (Fig 2.2 E).

Discussion

This chapter focused on understanding the working role of COL18A1 in the embryonic heart and how it may regulate coronary angiogenesis. In the previous chapter, we hypothesized that COL18A1 controls vasculature development as its presence is temporally correlated with periods of vasculature growth but not in the period of regeneration seen in neonates. Artificial overexpression of COL18A1-HA inhibits or prevents the proper placement of coronary endothelial cells. Gene expression data confirm that Col18a1 overexpression preserves a venous and coronary plexus phenotype in ECs. In addition, these ECs following overexpression of Col18a1 in the epicardium remained immature with an upregulation in proliferation and maintained venous cell markers while downregulating arterial markers. Furthermore, EPDCs appear to be immature and proliferative, with an upregulation in EMT regulation. Although EMT may be seen in the artificial COL18A1-HA overexpression group, we theorize that inhibition of cell differentiation may be responsible for the dysregulation in cell placement and coronary development. Further gene analysis of EMT-derived cells may provide further insight into the mechanism of COL18A1.

CONCLUSION

This study's main goal was the characterization of *Col18a1* and its role in the development of the heart. Through the work conducted in these experiments, we can conclude that *Col18a1* originates from both the endocardium and the epicardium. Epicardial-sourced *Col18a1* co-localizes with epicardial cells and migrates with these cells during EMT. In addition, *Col18a1* and endostatin, the cleaved C-terminal of *Col18a1*, increase in expression during embryonic development but remain stagnant during early neonatal heart growth. This finding supports the hypothesis that *Col18a1* and endostatin work as guidance markers for coronary angiogenesis. The artificial overexpression of COL18A1 further supports this finding by demonstrating that *Col18al* plays a key role in coronary angiogenesis. Endothelial cells exposed to COL18A1 maintained a more immature cellular phenotype in the presence of upregulated EMT. These results raise questions about the mechanism COL18A1 uses; does COL18A1 inhibit differentiation even in the presence of differentiation cues? Overall, this study provides a foundation for the role of *Col18a1* in the developing heart, which had not been previously described.

We would like to generate further replicates of the ex vivo approach to strengthen the conclusions gathered from this study. Manufacturing delays caused this limitation, and we present the data as correlative results without a clear indication of adenovirus arrivals. Future directions to further analyze the role of *Col18a1* in the development of coronary vasculature would require adopting an *in vivo Col18al* knockout model. Using a knockout mouse model, we hypothesize that without *Col18al* in the heart, endothelial cells would show increased differentiation of endothelial cells toward artery formation. Further analysis through bulk RNA sequencing will elucidate the role of *Col18al* in this genetic knockout model.

TABLES AND FIGURES

Primary Antibody (Dilution)	**Secondary Antibody (Dilution)**	**Tertiary Antibody (Dilution)**
Rabbit anti-GFP (1:200) Fisher Scientific Catalog No. TP401	Donkey anti-rabbit HRP (1: 2000) Jackson ImmunoResearch Catalog No. 711-035-152	Opal 570 (1:100) Akoya Biosciences Catalog No. FP1488001KT
Chicken anti-RFP (1:100) Rockland Catalog No. 600-901-379S	Donkey anti-chicken HRP (1: 2000 Dilution) Jackson ImmunoResearch Catalog No. 703-034-155	Opal 570 (1:100) Akoya Biosciences Catalog No. FP1488001KT
Mouse anti-Cardiac Troponin T (1:100) ThermoFisher Scientific Catalog No. MA5-12960	Donkey anti-mouse IgG Alexa Fluor 647 (1: 100 Dilution) Jackson ImmunoResearch Catalog No. 715-605-150	-
Rabbit anti-Endostatin (1:100) Millipore Sigma Catalog No. ABC60	Donkey anti-rabbit Biotin (1: 5000 Dilution) Jackson ImmunoResearch Catalog No. 711-065-152	Opal 570 (1:100) Akoya Biosciences Catalog No. FP1488001KT

Table 1: Antibodies used in Immunohistochemistry

Gene Target	Catalog #	Secondary	Dilution
eGFP	400281-C1	Opal 520	1:750
Col18a1	483801-C3	Opal 690	1:750
tdTomato	317041-C1	Opal 520	1:750
Col18a1	483801-C3	Opal 690	1:750
CDH5	312531-C1	Opal 520	1:750
Tcf21	508661-C2	Opal 570	1:750
Col18a1	483801-C3	Opal 690	1:750

Table 2: Gene Targets and dilution factors used in FISH; All gene targets were purchased from Advanced Cell Diagnostics

Primers for qRT-PCR		
Gene Target	Forward Primer	Reverse Primer
Col18a1	GGGGAAAGGATTC TTGCCTATG	GAAGGAACAGAGAG TAAACCGTG
Fibronectin	AGACCTGGGAAAA GCCCTACCAA	ACTGAAGCAGGTTTC CTCGGTTGT
Col18a1-HA Tag	GTCAGTGTTCCTGT CCTCC	CCAGATCTTCACCTG CCCA
Apln	TGAATCTGAGGCTC TGCGTG	ACATCAGTGGCACTC CACAA
Nrp1	CACAGTGGCACAGG TGATGA	ACCGTATGTCGGGAA CTCTGA
Nr2f2	ATCAACTAGCCCTG AGCCACC	CCGCCTTTTGTGTGTG CGAG
Cdk1	GGTCCGTCGTAACC TGTTGA	CCACACCGTAAGTAC CTTCTCC
Zeb2	AGGCGCGAGAGAA AGGGCAC	CCCGGTTCATCAGCA GCTCGG

Table 3: List of Primers used for qRT-PCR

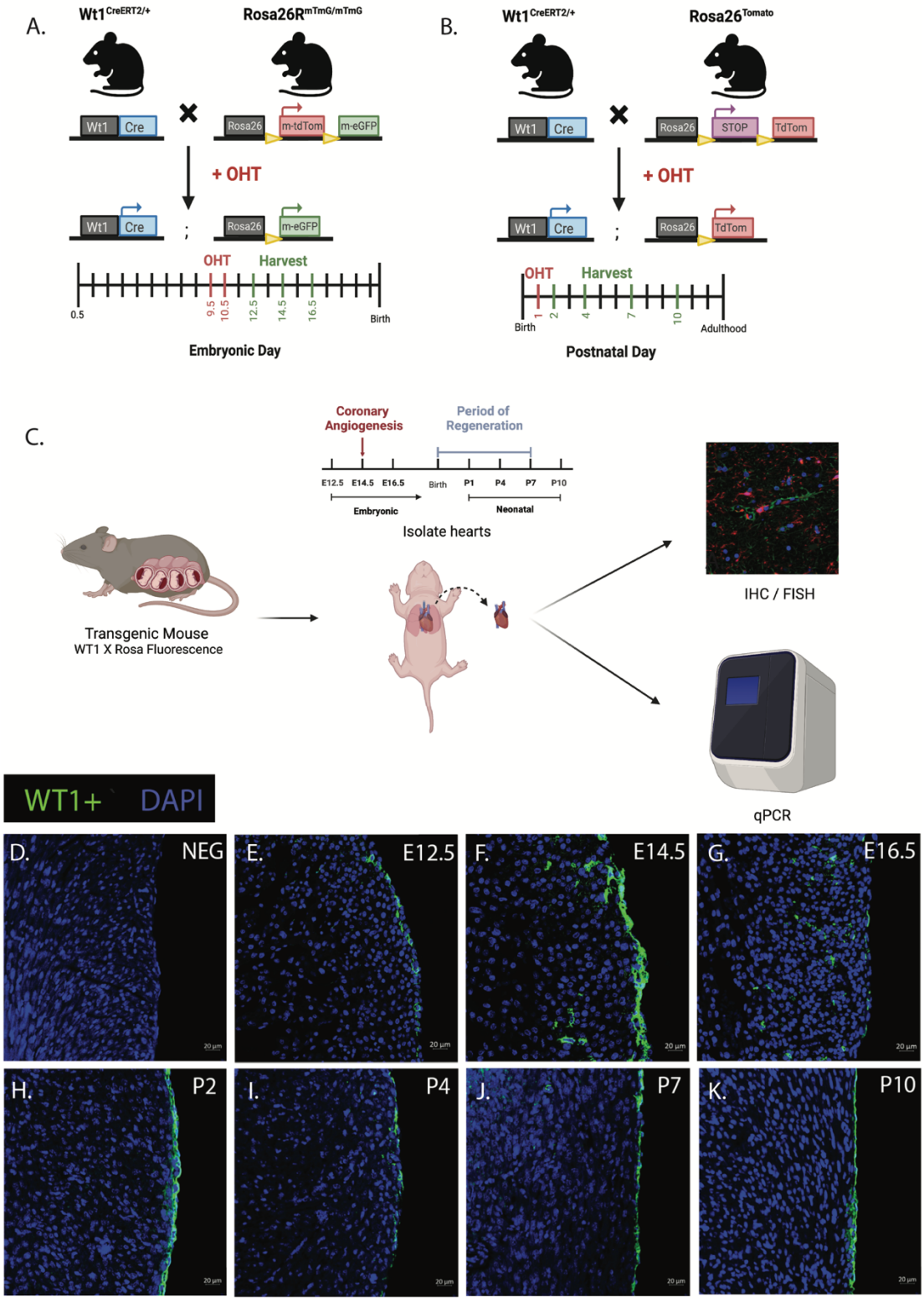

FIGURE 1.1 Experimental Protocol, Mouse Model, and visual confirmation of mouse model (A-B) Experimental strategy for lineage tracing EPDCs cells with $Wt1^{CreERT2/+}$;

Rosa26R$^{mTmG/mTmG}$ embryos (A) and Wt1$^{CreERT2/+}$; Rosa26^{tdTomato} neonates. 4-Hydroxytamoxifen was administered at E9.5 and E10.5 for embryos and harvested at E12.5, E14.5, and E16.5(A). Neonates had 4-Hydroxytamoxifen administered at P1 and were harvest at P2, P4, P7, and P10 (B). **(C)** Schematic of experimental protocol. **(D-G)** Representative confocal images from Wt1$^{CreERT2/+}$; Rosa26R$^{mTmG/mTmG}$ embryonic mouse hearts harvested at E12.5, E14.5, and E16.5. Wt1+ cells are shown in green. DAPI was used to stain for cell nuclei (blue). Each experiment was replicated 3 times and demonstrated similar results. Scale bar = 20μm. **(H-K)** Representative confocal images from Wt1$^{CreERT2/+}$; Rosa26^{tdTomato} neonatal mouse hearts harvested at P2, P4, P7, and P10. Wt1+ cells are shown in green. DAPI was used to stain for cell nuclei (blue). Each experiment was replicated 3 times and demonstrated similar results. Scale bar = 20μm.

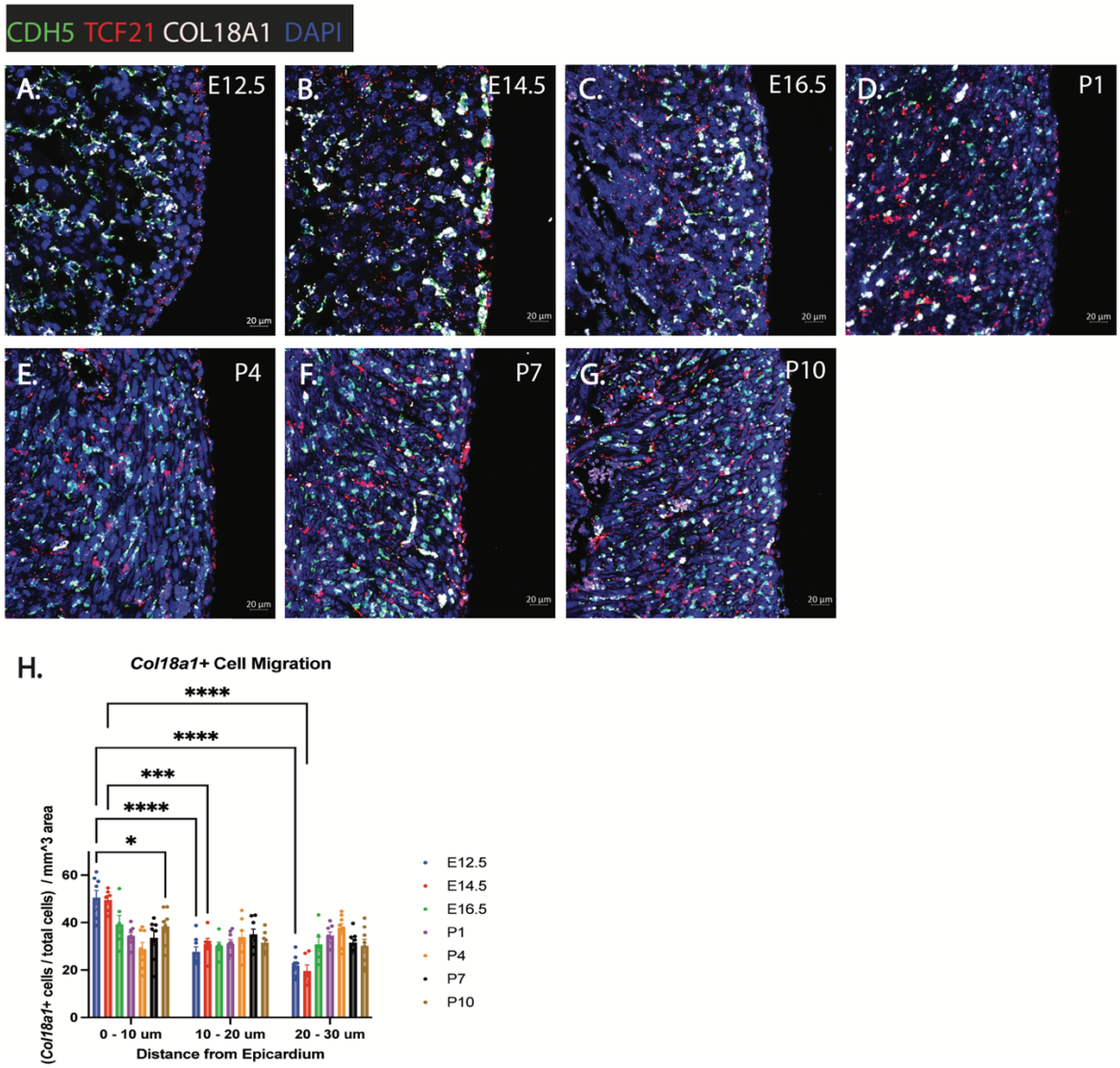

Figure 1.2: *Col18a1* expression and migration patterns; (A-G) Representative confocal images from Wt1$^{CreERT2/+}$; Rosa26R$^{mTmG/mTmG}$ embryonic mouse hearts harvested at E12.5, E14.5, and E16.5 (A-C) and Wt1$^{CreERT2/+}$; Rosa26^{Tomato} neonatal mouse hearts harvested at P2, P4, P7, and P10 (D-G). Cdh5+ cells are shown in green (CDH5 is a marker for VE-cadherin; a canonical marker of endothelial cells). Tcf21+ cells are shown in red (a marker for epicardial cells and epicardial-derived fibroblasts). Col18a1+ cells are shown in white. DAPI was used to stain for cell nuclei (blue). Each experiment was replicated 3 times and demonstrated similar results. Scale bar = 20µm. **(H)** Quantification of *Col18a1*+ Cell migration visualized in A-G across all replicates. Data are presented as mean values ± SEM. Statistical significance was determined by a two-way ANOVA.

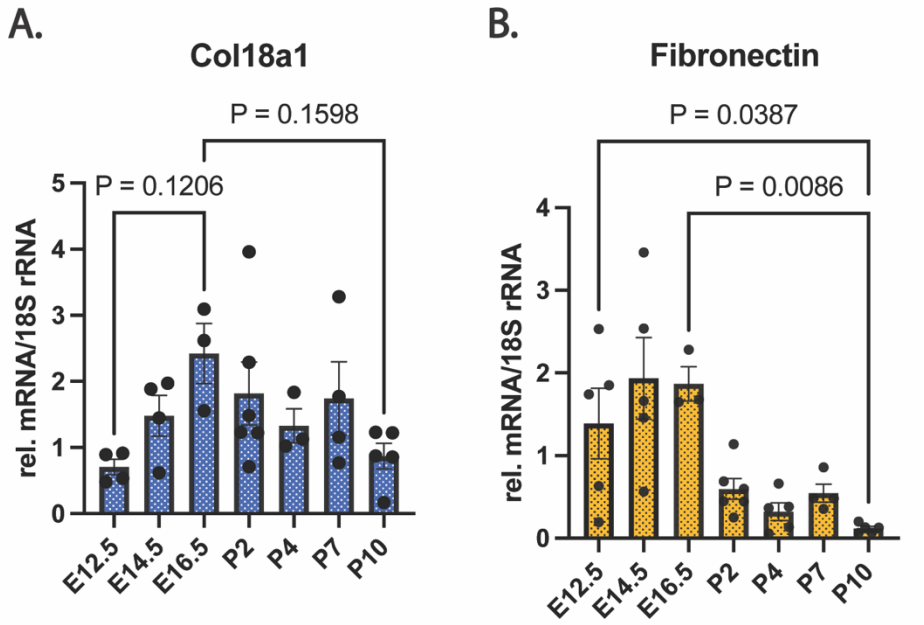

Figure 1.3: Gene analysis of Col18a1 and FN; (A–B) Expression of endogenous genes taken from whole heart samples and validated by qRT-PCR. Values are represented as a fold change in expression relative to the 18S gene. Data are presented mean values ± SEM. Statistical significance was determined by a one-way ANOVA.

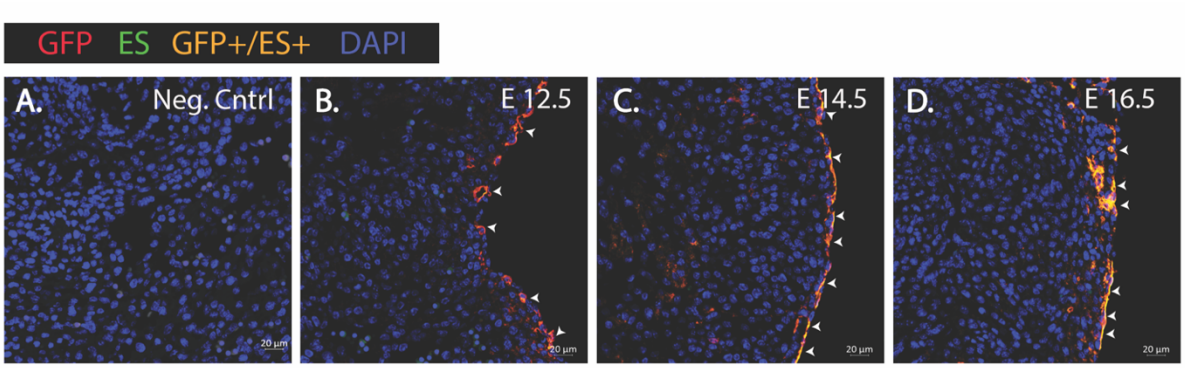

Figure 1.4: Endostatin Placement of Embryonic and Neonatal Mice; (A-D) Representative confocal images from $Wt1^{CreERT2/+}$; $Rosa26R^{mTmG/mTmG}$ embryonic mouse hearts harvested at E12.5, E14.5, and E16.5. GFP+ cells are shown in red. Endostatin is shown in green. Colocalization of GFP+/ES+ is shown in orange and indicated with arrow heads. DAPI was used to stain for cell nuclei (blue). Each experiment was replicated 3 times and demonstrated similar results. Scale bar = 20µm.

Primary Antibody (Dilution)	Secondary Antibody (Dilution)
Rabbit anti-ERG (1:100) Abcam Catalog No. Ab115555	Donkey anti-rabbit Cy3 (1:100) Jackson ImmunoResearch Catalog No. 705-165-147
Rabbit-HA Tag (1:100) Cell Signaling Technology Catalog No. C29F4	Donkey anti-rabbit 647 (1:100) Jackson ImmunoResearch Catalog No. 711-605-152

Table 4: Antibodies used in Immunohistochemistry

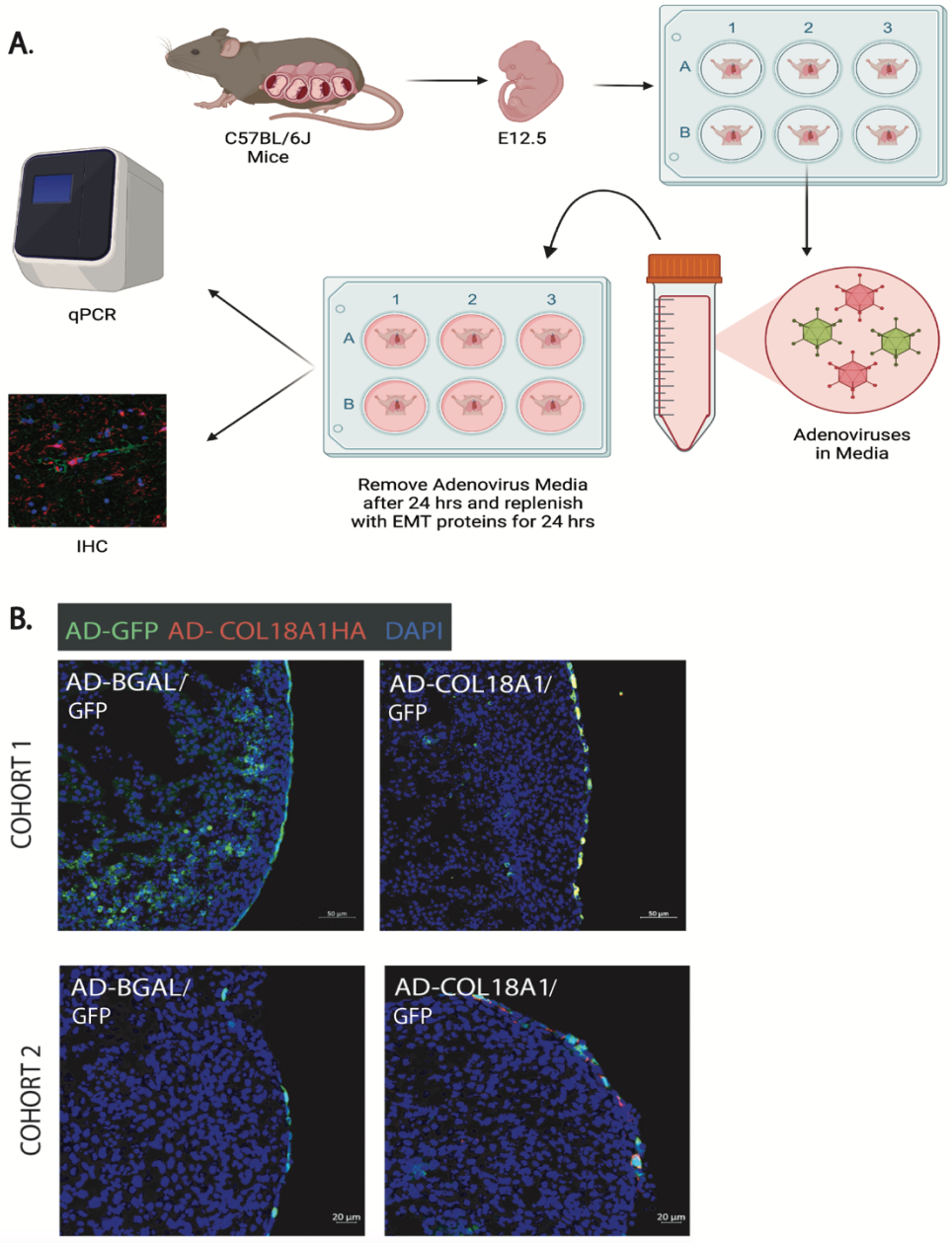

Figure 2.1: Experimental Protocol Schematic and Visual Confirmation of Overexpression; (A) Experimental schematic for artificial overexpression with adenoviruses. **(B)** Representative confocal images from C57BL/6J mice following adenovirus overexpression for 24 hours, followed with 24 hours with EMT inducing proteins. Hearts exposed to AD-GFP and AD-BGal are shown in the left column. Hearts exposed to AD-GFP and AD-COL18A1-HA are shown in the right column. Cells infected with AD-GFP are shown in green. Cells infected with AD-COL18A1-HA are shown in red. DAPI was used to stain for cell nuclei (blue). Each experiment was replicated 3 times and demonstrated similar results. Scale bar = 20µm.

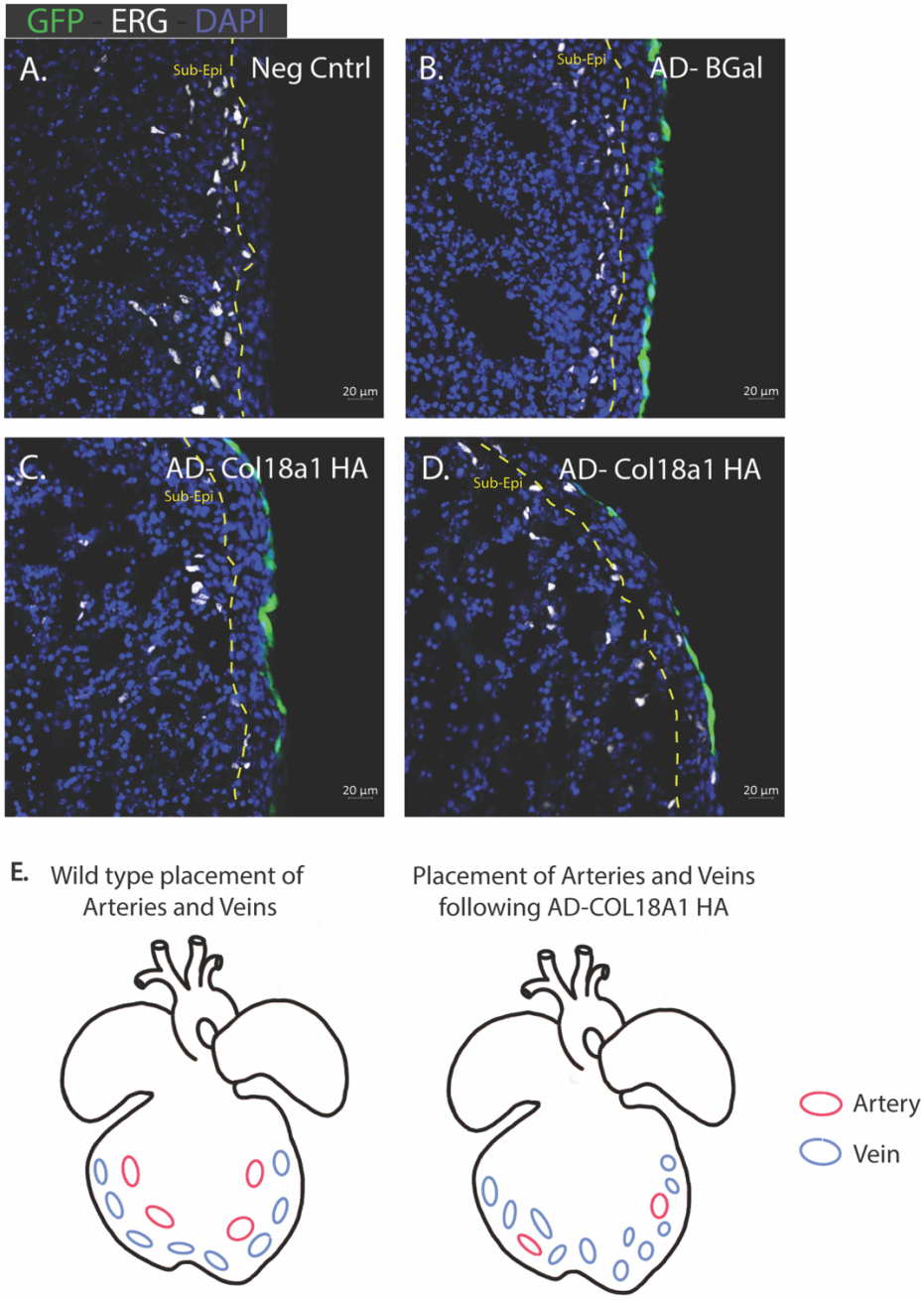

Figure 2.2: ERG placement and Coronary vasculature Placement Theory; (A–D) C57BL/6J embryonic hearts were exposed to AD-GFP and AD-COL18A1 HA or AD-GFP and AD-BGal to induce overexpression for 24 hours, followed with 24 hours with EMT inducing proteins. Representative confocal images demonstrate EC (shown by ERG+) cell placement. The sub-epicardium (sub-epi) region is identified with a yellow dashed line. Cells infected with AD-GFP are shown in green. ERG+ cells are shown in white. DAPI was used to stain for cell nuclei (blue). Each experiment was replicated 3 times and demonstrated similar results. Scale bar = 20µm. **(E)** Schematic of vasculature development and hypothesized influence of AD-COL18A1 HA on vasculature development.

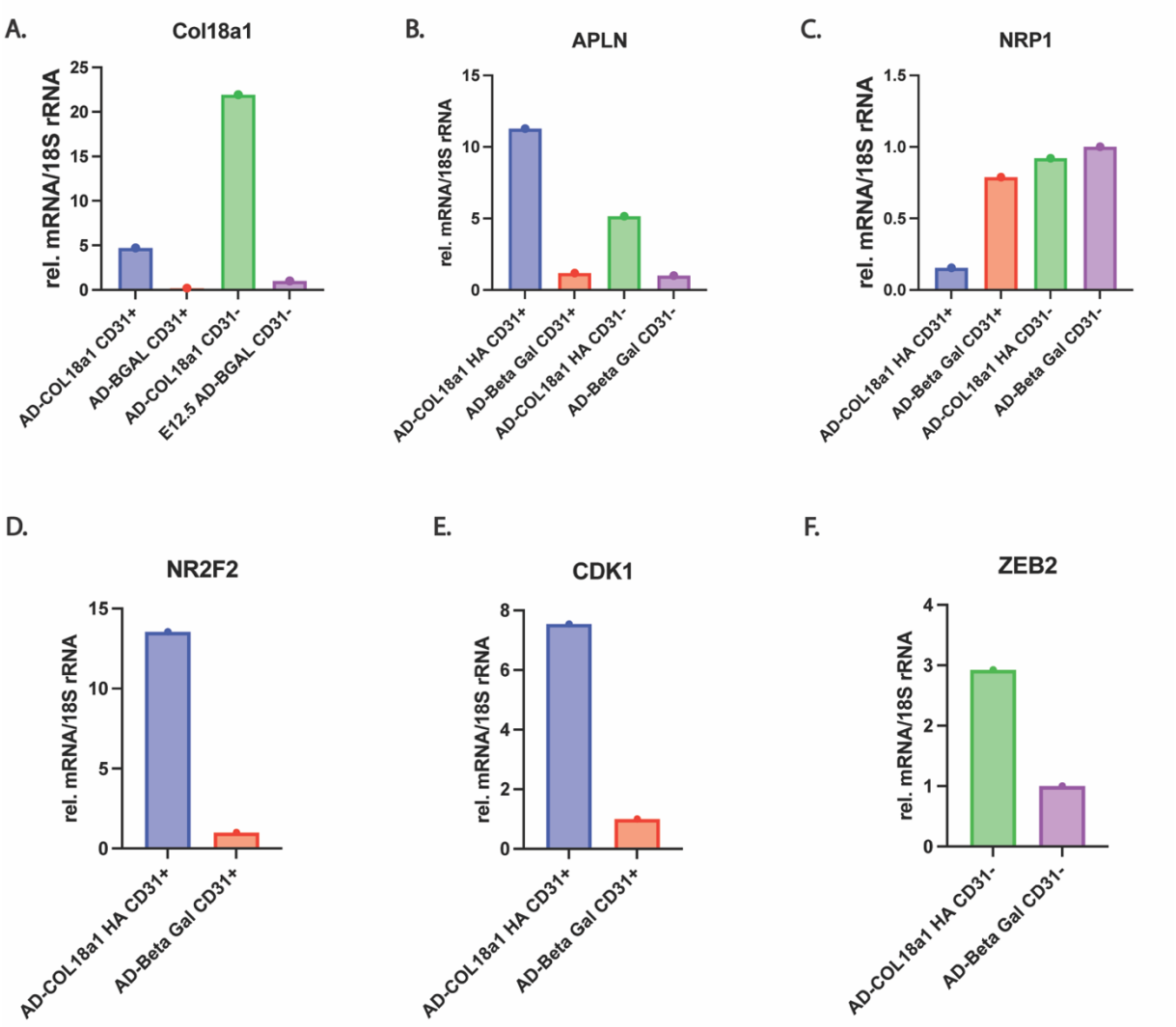

Figure 2.3: Gene analysis of Col18a1, EMT, Cell Cycle and EC Specification; (A–F) C57BL/6J embryonic hearts were exposed to AD-COL18A1-HA or AD-BGal to induce overexpression for 24 hours, followed with 24 hours with EMT inducing proteins. CD31-positive and negative cells were sorted via FACS. Relative expression of genes (*Col18a1*, gene of interest; *Apln*, sinus vinous marker; *Nrp1*, arterial marker; *Nr2f2*, venous marker; *Cdk1*, cell cycle and proliferation marker; *Zeb2*, EMT regulation marker) were validated by qRT-PCR. Values are represented as a fold change in expression relative to the 18S rRNA control, as there is little variation and is highly abundant.

REFERENCES

1. Bloomekatz J, Singh R, Prall OW, Dunn AC, Vaughan M, Loo CS, Harvey RP, Yelon D. Platelet-derived growth factor (PDGF) signaling directs cardiomyocyte movement toward the midline during heart tube assembly. Elife. 2017 Jan 18;6:e21172. doi: 10.7554/eLife.21172. PMID: 28098558; PMCID: PMC5298878.
2. Cano, A., Pérez-Moreno, M., Rodrigo, I. et al. The transcription factor Snail controls epithelial–mesenchymal transitions by repressing E-cadherin expression. Nat Cell Biol 2, 76–83 (2000). https://doi.org/10.1038/35000025
3. CDC Wonder. (2023, January 11). Multiple cause of death data on CDC Wonder. Centers for Disease Control and Prevention. https://wonder.cdc.gov/mcd.html
4. Compton LA, Potash DA, Mundell NA, Barnett JV. Transforming growth factor-beta induces loss of epithelial character and smooth muscle cell differentiation in epicardial cells. Dev Dyn. 2006 Jan;235(1):82-93. doi: 10.1002/dvdy.20629. PMID: 16258965.
5. Donovan MF, Cascella M. Embryology, Weeks 6-8. [Updated 2022 Oct 10]. In: StatPearls [Internet]. Treasure Island (FL): StatPearls Publishing; 2023 Jan-. Available from: https://www.ncbi.nlm.nih.gov/books/NBK563181/
6. Georg Ertl , Stefan Frantz, Healing after myocardial infarction, Cardiovascular Research, Volume 66, Issue 1, April 2005, Pages 22–32, https://doi.org/10.1016/j.cardiores.2005.01.011
7. Kovacic JC, Mercader N, Torres M, Boehm M, Fuster V. Epithelial-to-mesenchymal and endothelial-to-mesenchymal transition: from cardiovascular development to disease. Circulation. 2012 Apr 10;125(14):1795-808. doi: 10.1161/CIRCULATIONAHA.111.040352. PMID: 22492947; PMCID: PMC3333843.

8. Lamouille S, Xu J, Derynck R. Molecular mechanisms of epithelial-mesenchymal transition. Nat Rev Mol Cell Biol. 2014 Mar;15(3):178-96. doi: 10.1038/nrm3758. PMID: 24556840; PMCID: PMC4240281.
9. Lavine KJ, Yu K, White AC, Zhang X, Smith C, Partanen J, Ornitz DM. Endocardial and epicardial derived FGF signals regulate myocardial proliferation and differentiation in vivo. Dev Cell. 2005 Jan;8(1):85-95. doi: 10.1016/j.devcel.2004.12.002. PMID: 15621532.
10. Moise, Alexander R., et al. "Development of the Coronary System: Perspectives for Cell Therapy from Precursor Differentiation." Endothelium and Cardiovascular Diseases, 2018, pp. 11–22., https://doi.org/10.1016/b978-0-12-812348-5.00002-7.
11. Moulton, Karen S., et al. "Loss of Collagen XVIII Enhances Neovascularization and Vascular Permeability in Atherosclerosis." Circulation, vol. 110, no. 10, 2004, pp. 1330–1336., https://doi.org/10.1161/01.cir.0000140720.79015.3c.
12. O'Reilly, M S et al. "Endostatin: an endogenous inhibitor of angiogenesis and tumor growth." Cell vol. 88,2 (1997): 277-85. doi:10.1016/s0092-8674(00)81848-6 5
13. Rodríguez, Patricia, et al. "The Non-Canonical Notch Ligand DLK1 Exhibits a Novel Vascular Role as a Strong Inhibitor of Angiogenesis." Cardiovascular Research, vol. 93, no. 2, 2011, pp. 232–241., https://doi.org/10.1093/cvr/cvr296.

14. Porrello ER, Mahmoud AI, Simpson E, Hill JA, Richardson JA, Olson EN, Sadek HA. Transient regenerative potential of the neonatal mouse heart. Science. 2011 Feb 25;331(6020):1078-80. doi: 10.1126/science.1200708. PMID: 21350179; PMCID: PMC3099478.

15. Quijada, P., Trembley, M. A., & Small, E. M. (2020). The role of the epicardium during Heart Development and Repair. Circulation Research, 126(3), 377–394. https://doi.org/10.1161/circresaha.119.315857

16. Quijada, P., Trembley, M.A., Misra, A. et al. Coordination of endothelial cell positioning and fate specification by the epicardium. Nat Commun 12, 4155 (2021). https://doi.org/10.1038/s41467-021-24414-z

17. Ramchandran, Ramani et al. ``Cellular actions and signaling by endostatin.” Critical reviews in eukaryotic gene expression vol. 12,3 (2002): 175-91. doi:10.1615/critreveukaryotgeneexpr.v12.i3.20

18. Red-Horse, K., Ueno, H., Weissman, I. et al. Coronary arteries form by developmental reprogramming of venous cells. Nature 464, 549–553 (2010). https://doi.org/10.1038/nature08873

19. Rhee, S., Wu, J.C. Vein to artery: the first arteriogenesis in the mammalian embryo. Cell Res 32, 325–326 (2022). https://doi.org/10.1038/s41422-022-00629-7

20. Sabra M, Karbasiafshar C, Aboulgheit A, Raj S, Abid MR, Sellke FW. Clinical Application of Novel Therapies for Coronary Angiogenesis: Overview, Challenges, and Prospects. Int J Mol Sci. 2021 Apr 2;22(7):3722. doi: 10.3390/ijms22073722. PMID: 33918396; PMCID: PMC8038234.

21. Smith, C. L., Baek, S. T., Sung, C. Y., & Tallquist, M. D. (2011). Epicardial-derived cell epithelial-to-mesenchymal transition and fate specification require PDGF receptor signaling. Circulation Research, 108(12). https://doi.org/10.1161/circresaha.110.235531

22. Tian, X., Pu, W. T., & Zhou, B. (2015). Cellular origin and developmental program of coronary angiogenesis. Circulation Research, 116(3), 515–530. https://doi.org/10.1161/circresaha.116.305097

23. Trembley MA, Velasquez LS, de Mesy Bentley KL, Small EM. Myocardin-related transcription factors control the motility of epicardium-derived cells and the maturation of coronary vessels. Development. 2015 Jan 1;142(1):21-30. doi: 10.1242/dev.116418. PMID: 25516967; PMCID: PMC4299137.

24. Tsao, C. W., Aday, A. W., Almarzooq, Z. I., Alonso, A., Beaton, A. Z., Bittencourt, M. S., Boehme, A. K., Buxton, A. E., Carson, A. P., Commodore-Mensah, Y., Elkind, M. S. V., Evenson, K. R., Eze-Nliam, C., Ferguson, J. F., Generoso, G., Ho, J. E., Kalani, R., Khan, S. S., Kissela, B. M., … Martin, S. S. (2022). Heart disease and stroke statistics—2022 update: A report from the American Heart Association. Circulation, 145(8). https://doi.org/10.1161/cir.0000000000001052

25. Visse, Robert, and Hideaki Nagase. "Matrix Metalloproteinases and Tissue Inhibitors of Metalloproteinases." Circulation Research, vol. 92, no. 8, 2003, pp. 827–839., https://doi.org/10.1161/01.res.0000070112.80711.3d.

26. Wu B, Zhang Z, Lui W, Chen X, Wang Y, Chamberlain AA, Moreno-Rodriguez RA, Markwald RR, O'Rourke BP, Sharp DJ, Zheng D, Lenz J, Baldwin HS, Chang CP, Zhou B. Endocardial cells form the coronary arteries by angiogenesis through myocardial-

endocardial VEGF signaling. Cell. 2012 Nov 21;151(5):1083-96. doi: 10.1016/j.cell.2012.10.023. PMID: 23178125; PMCID: PMC3508471.

27. Wu, X., Reboll, M. R., Korf-Klingebiel, M., & Wollert, K. C. (2020). Angiogenesis after acute myocardial infarction. Cardiovascular Research, 117(5), 1257–1273. https://doi.org/10.1093/cvr/cvaa287

28. Xu J, Lamouille S, Derynck R. TGF-beta-induced epithelial to mesenchymal transition. Cell Res. 2009 Feb;19(2):156-72. doi: 10.1038/cr.2009.5. PMID: 19153598; PMCID: PMC4720263.